

## Synthesis and Characterization of Activated Carbon from Hydrothermally Banana Empty Fruit Bunch for Adsorption of Pb(II) and Cr(VI) in Aqueous Solution

ALLWAR ALLWAR\*, KLANA WIJAYA A. SYAMSUDIN, RENI BANOWATI ISTININGRUM and NURCAHYO IMAM PRAKOSO

Department of Chemistry, Faculty of Mathematics and Natural Sciences, Universitas Islam Indonesia, Kampus Terpadu UII, Jalan Kaliurang, Km 14.5, Besi, Sleman, Yogyakarta 55584, Indonesia

\*Corresponding author: E-mail: [allwar@uui.ac.id](mailto:allwar@uui.ac.id)

Received: 20 February 2018;

Accepted: 10 May 2018;

Published online: 31 May 2018;

AJC-18946

Activated carbon was synthesized from banana empty fruit bunch using phosphoric acid activation under hydrothermal process and used its effectiveness was examined for adsorption of Pb(II) and Cr(VI) ions in aqueous solution. The plot of nitrogen adsorption desorption isotherm provides the combination of Type II and IV isotherms with wide hysteresis loop, relating to highly mesoporous structure. The morphological surface shows an irregular or unsmooth, and most of the pores are closed. The FTIR spectrum shows that activated carbon has oxygen-containing functional groups. Adsorption capacity was observed with different parameters such as pH of the solution, adsorbent dosage, contact time and concentration of adsorbate. Equilibrium adsorptions were evaluated using the Freundlich and Langmuir isotherm. The Langmuir shows more favourable than Freundlich isotherm with correlation coefficient,  $R^2$  of 0.9767 and 0.9693 for Pb(II) and Cr(VI) ions, respectively. The results of this work proved that the banana empty fruit bunch activated is effectively used as adsorbent for adsorption of the metal ions from aqueous solution.

**Keywords:** Banana empty fruit bunch, Activated carbon, Hydrothermal, Freundlich and Langmuir, Pb(II) and Cr(VI) ions.

### INTRODUCTION

Recently, ecological issues concerning of the industrial waste and by-product of human activities will be important area to be discussed to solve a great problem worldwide. There has been an increasing the environmental contamination caused by heavy metal such as nickel, lead, mercury, chromium, arsenic, *etc.* [1,2]. Heavy metal is highly soluble in aquatic environments and easily found in water effluent and soil. The source of metal ion is from the result of electroplating, conversion-coating, pigment manufacturing, anodizing cleaner and milling processes [3,4]. Once metal ion is absorbed and accumulated beyond the permitted concentration in living organisms, it will cause a serious disorder health. Some technologies have been proposed to minimize heavy metal ion prior to discharge in environment such as adsorption, precipitation, membrane filter, ion-exchange, electrochemical deposition and bioleaching remediation [5,6]. Adsorption technique might have the most popular process for removal of heavy metal ion in solution. The advantages of adsorption techniques are that they are easily produced and have highly adsorption capacity. Adsorption process can be done by various types of adsorbent. Adsorbent is a highly porous material with excellent physical and chemical properties like high surface area, pore volume and

pore size distribution including various types of surface chemistry.

Activated carbon is one of type adsorbents that can be prepared from highly carbonaceous compound such as agricultural waste, industrial by-product and natural materials. Adsorbent activated carbon is widely used in many applications in industries such as recovery the solvents through separation and purification process. Recently, the usage of activated carbon steadily increased with increasing the number of industries. It is necessary to explore the new raw material sources for activated carbon production. Agricultural waste would be better alternative precursor for activated carbon productions such as apple waste, coconut shell, banana empty fruit bunch, *etc.* due to its availability in large quantity [7].

Banana is an edible fruit that one of the most popular fruit all over the world. It is considered to have a good taste, rich of vitamins and minerals. A banana is usually consumed in fresh or processed to other types of foods such as cake, juice, biscuit, wine *etc.* Banana can be separated into trunk, leaves, fruit and empty fruit bunch. Banana empty fruit bunch may not be used for many purposes and are mostly dumped as solid waste at open area. It may cause a real environmental problem. It is significant to find a method for protection of the clean ecosystem and enhance toward zero pollution. Previous

works reported that banana empty fruit bunch consisting of cellulose (8.30 %), hemicellulose (21.23 %) and lignin (19.06 %) have been used as alternative raw material for preparation of activated carbon [8]. However, the activated carbon from banana empty fruit bunch may not be completely studied, and it is needed an exploration for its better quality and application.

The objectives of the present study are to prepare activated carbon from banana empty fruit bunch using phosphoric acid activation and under hydrothermal process. Analysis of its physical and chemical properties is determined by the Pore Size Analyzer Quantachrome NOVA 2200e, Fourier transform infrared spectroscopy (FTIR) and scanning electron microscopy-energy dispersive X-ray spectroscopy (SEM-EDS). Adsorption capacity of activated carbon is evaluated for adsorption of Pb(II) and Cr(VI) in solution. The efficiency of activated carbon is investigated by different parameters such as pH solution, adsorbent dosage, concentration of metals and contact time. Adsorption capacity of metal ions is determined by atomic absorption spectrophotometer (AAS). Equilibrium adsorption is determined by the Freundlich and Langmuir isotherm models.

## EXPERIMENTAL

Banana empty fruit bunches (BEFB) as a raw material sample was collected at around the banana seller and cut down to a small pieces in the range of 0.5-1.0 mm. Phosphoric acid, nitric acid, lead(II) nitrate and potassium chromate were supplied by Merck.

**Preparation of activated carbon:** Activated carbon was synthesized by chemical activation using hydrothermal process. Approximately, 500 g banana empty fruit bunch sample was impregnated with 500 mL of 10 % phosphoric acid. The mixture was refluxed at 80 °C for 6 h. Thereafter, the mixture was filtered and washed several times with hot distilled water to remove excess acid and increase the pH 6-7 [9]. Sample was placed in reactor hydrothermal and added 250 mL distilled water. The hydrothermal reactor was slowly heated at 250 °C for 3 h. After cooling down, sample was taken out and immersed into 3 M nitric acid for 3 h. To obtain activated carbon, the mixture was filtered and dried in oven at 120 °C for 24 h and kept for further analysis.

### Characterization of activated carbon

**Nitrogen adsorption-desorption isotherm:** Pore structures of activated carbon were analyzed by Quantachrome surface area analyzer. The BET surface area, total pore volume, micropore volume and pore size distribution were calculated by the nitrogen adsorption-desorption isotherms data. The specific surface areas were determined with BET method at relative pressure in the range of 0.05-0.3. Micropore volume was calculated from Dubinin-Radushkevich (DR) method, while total pore volume was obtained from the highest relative pressure ( $p/p_0 = 0.99$ ). Pore size distribution was estimated from Barret-Joyner-Halenda (BJH) method.

**Moisture and ash content of activated carbon:** Moisture content of activated carbon was calculated by following method. Approximately, 0.5 g of activated carbon was transferred into tarred crucible. The sample was dried into an oven at 120 °C for 3 h. Thereafter, the sample was kept in desiccators and

immediately weight to prevent air or moisture adsorption. Moisture percentage content was calculated using eqn. 1.

$$\text{Moisture content (\%)} = \frac{A - B}{B} \times 100 \quad (1)$$

where, A = weight of final sample (g); B = weight of initial sample (g).

In order to determine ash content, 0.5 g of activated carbon was transferred into tarred crucible and moderately heated up to 600 °C for 4 h. The sample was cooled in desiccators and immediately weight to obtain weight loss. Calculation of percentage of ash content was obtained by eqn. 2 [10].

$$\text{Ash content (\%)} = \frac{\text{Weight of ash (g)}}{\text{Weight of initial dried sample (g)}} \times 100 \quad (2)$$

**Functional group on the activated carbon:** Functional group on the surface of activated carbon was carried out using Fourier transform infrared spectrometer (FTIR) in the range of 4000-400  $\text{cm}^{-1}$ . A pellet of activated carbon was prepared by mixing with an equivalent quantity of dried KBr under small hydraulic pressed at 8 N.

**Morphology of the activated carbon:** Microstructure and elemental composition of activated carbon were determined by scanning electron microscopy (SEM) and energy dispersive spectrometer (EDS).

**Parameters effecting adsorption process of activated carbon:** Adsorption of metal ions, Pb(II) and Cr(IV) was carried out by batch sorption experiments and tested with some influenced factors such as pH solution, contact time, concentration and adsorbent dosage. Adsorption capacity was measured at different pH under acid and basic solution in the range of pH 2-10. The effects of adsorbent dosage were carried out at different mass in the range of 0.5-2.0 g. The contact times were conducted for period of times in the range of 15-60 min. The initial concentrations of metal ions were carried out in the range of 100-200 mg/L. The capacity adsorption was determined by atomic absorption spectrophotometer (AAS) analysis. Adsorption equilibrium isotherm was evaluated by the Freundlich and Langmuir isotherm models.

**Adsorption isotherms study of activated carbon:** Equilibrium adsorption was studied by the sorption isotherm data. Analysis of adsorption was observed from interaction between adsorbate and adsorbent which is called adsorption capacity. The sorption process can be conducted in two phases; monolayer and multilayer. Two types of isotherm have been well known as Freundlich and Langmuir isotherm models. The Freundlich isotherm model occurred on the multilayer on the heterogeneous pores: meso- and macropores or combination both types of pores. While, the Langmuir isotherm is considered as monolayer adsorption on the surface occurring on the homogeneous micropore with no transmigration of adsorbate in plane of surface.

For Langmuir isotherm model is expressed from linear based as eqn. 3:

$$\frac{C_e}{q_e} = \frac{1}{K_L q_m} + \frac{C_e}{q_m} \quad (3)$$

The value of  $q_e$  is the adsorption capacity of metals at equilibrium (mg/g). The values of  $q_m$  (mg/g) and  $K_L$  (L/mg)

are the Langmuir isotherm constant related to the maximum adsorption and energy adsorption, respectively. The Langmuir isotherm model was calculated from linear plot of specific adsorption ( $C_e/q_e$ ) versus equilibrium concentration ( $C_e$ ) [11].

The Freundlich isotherm model is expressed as eqn. 1.

$$q_e = K_F C_e^{1/n} \tag{4}$$

Linear parameter can be expressed by taking logarithms for determination of  $K_F$  and  $n$  by the following eqn. 2.

$$\log q_e = \log K_F + \frac{1}{n} \log C_e \tag{5}$$

A plot of  $\log q_e$  versus  $\log C_e$  gives a straight line. The values of  $K_F$  and  $1/n$  are the Freundlich isotherm constant related to the adsorption capacity and adsorption intensity, respectively which can be estimated from the intercept and slop. The value of adsorption intensity shows the favourability of adsorption [12,13].

**RESULTS AND DISCUSSION**

**Nitrogen adsorption-desorption isotherm:** Determination of porous structure was well determined by the surface area analyzer at the range of relative pressure 0.005-0.99. The plot of nitrogen adsorption-desorption isotherms at -196 °C exhibits typical combination of Type II and Type IV isotherms, relating with narrow- and wide-mesoporous activated carbon is presented in Fig. 1. The appearance of hysteresis loop at relative pressure above 0.4 indicates a process of the filling or emptying of mesopores as multilayer adsorption on the pores. Applying the adsorption desorption isotherms data revealed the extension of well-developed mesoporous pores. Specific surface area is usually estimated by the BET theory at the correlation coefficient,  $r = 0.99$  and at relative pressure in the range of 0.05-0.30. However, the Langmuir surface area is usually used to estimate the micropores and show the behaviour of gaseous particles on monolayer the surface. The Langmuir surface area is calculated in according with the monolayer capacity at narrow range of relative pressure below 0.05. In this work, the Langmuir surface area is taken at wide relative pressure in the range of 0.005-0.3. This reason assumed that the Langmuir surface area shows untrue values with higher its surface area compared to the BET surface area as shown in Table-1.

Capillary condensation of pore material related with the filling and emptying of meso- and macropores. These phenomena are generally responsible to the typical Type IV isotherm with the presence of hysteresis loop as multilayer pores. A plot of pore size distribution of activated carbon based on the Barret, Joyner and Halenda (BJH) method is shown in Fig. 2. The maximum peak of activated carbons is shown at around 20 Å and decreased to 500 Å on the pore radius. The results indicated that activated carbon consists of wide range of mesopores.

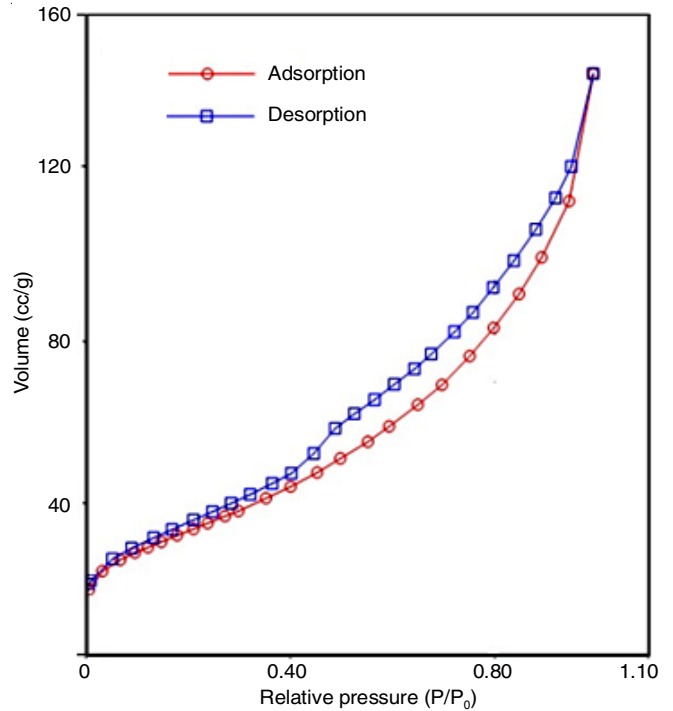


Fig. 1. Nitrogen adsorption desorption isotherm of activated carbon

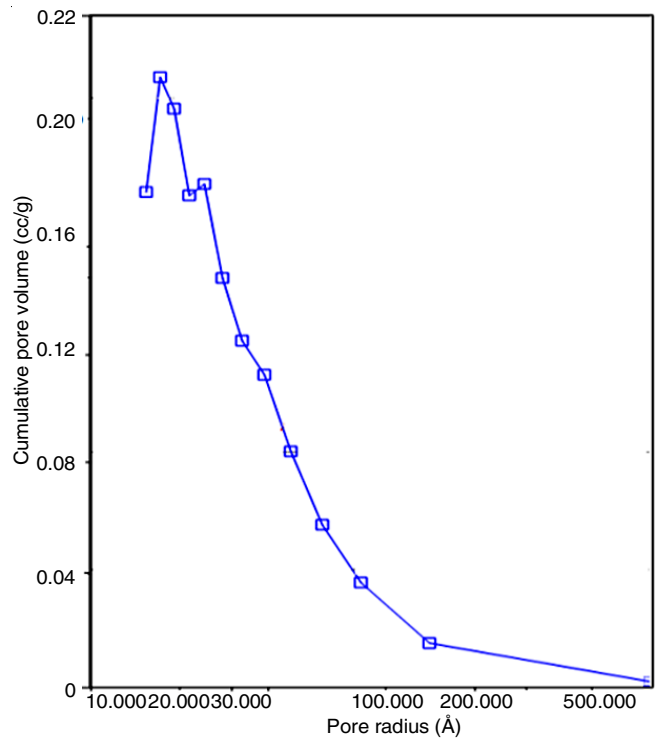


Fig. 2. Pore size distribution of activated carbon

This result is consistence with the typical isotherm model of Type IV and hysteresis loop. These reasonable reasons to conclude that the activated carbon prepared from banana empty

TABLE-1 TEXTURAL PROPERTIES OF ACTIVATED CARBON						
Langmuir surface area (m <sup>2</sup> /g)	BET multipoint surface area (m <sup>2</sup> /g)	DR micropore volume (cc/g)	BJH adsorption pore radius (Å)	DA pore radius (Å)	Total pore volume at P/P <sub>0</sub> 0.99 (cc/g)	Average pore radius (Å)
166.54	113.10	0.052	17.136	8.90	0.23	40.20

fruit bunch associate with multilayer pore with mesopores size distribution.

**Morphology of the activated carbon:** The surface morphology of activated carbon determined by SEM-EDS is shown in Fig. 3. The micrograph of external surface indicated an irregular formation because the surface was cracked into small particles during hydrothermal process and closed the mouth of pores. The elemental analysis of activated carbon is presented in Fig. 4. The result of EDX shows the elemental analysis obtained on the activated carbon. The high elements existed on the surface are carbon 44.36 %, oxygen 27.34 %, nitrogen 12.04 % and other unwanted particles in small quantity.

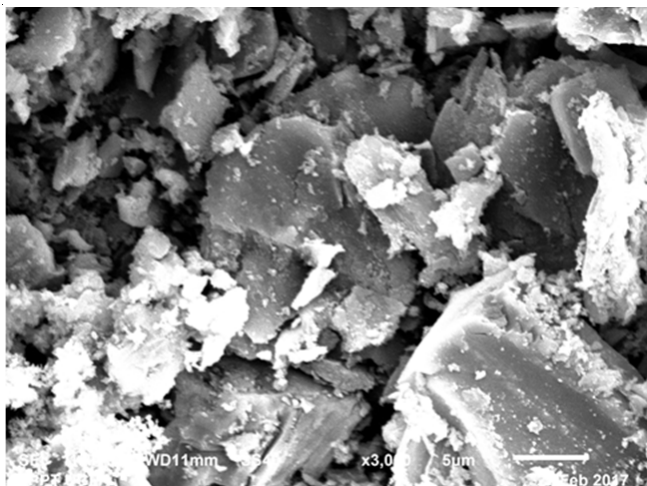


Fig. 3. SEM image of activated carbon

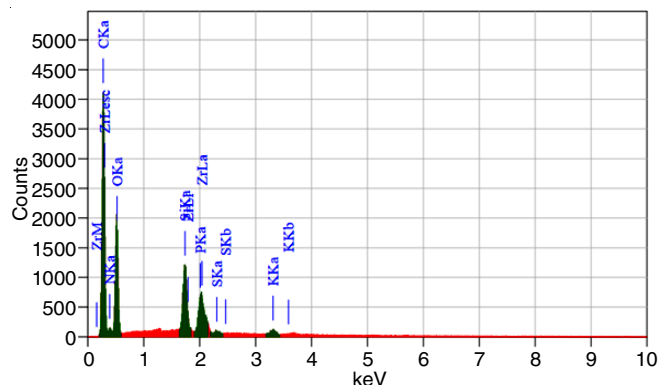


Fig. 4. Elemental analysis of activated carbon

**Functional group analysis:** The FTIR is one of important techniques to determine the functional group attached on the surface of activated carbon. The spectra of activated carbon obtained at wave number in the range of 4000-400  $\text{cm}^{-1}$  are shown in Fig. 5. There are two models of spectra: A) the spectrum of activated carbon, B) the spectrum after treatment with nitric acid. A weak peak at 3177  $\text{cm}^{-1}$  is assigned to O-H stretching vibration in hydroxyl group, which is overlapped with vinyl and acrylic C-H groups, aliphatic hydrocarbon. A band at 1623  $\text{cm}^{-1}$  is attributed double bond region C=C skeletal stretching. A weak peak at 1572  $\text{cm}^{-1}$  appeared after nitric acid treatment is usually ascribed to double bond C=C stretching in aromatic ring which overlap with C=O stretching in the carbonyl, ketone and carboxylate group in acid treatment. Appearance of a strong

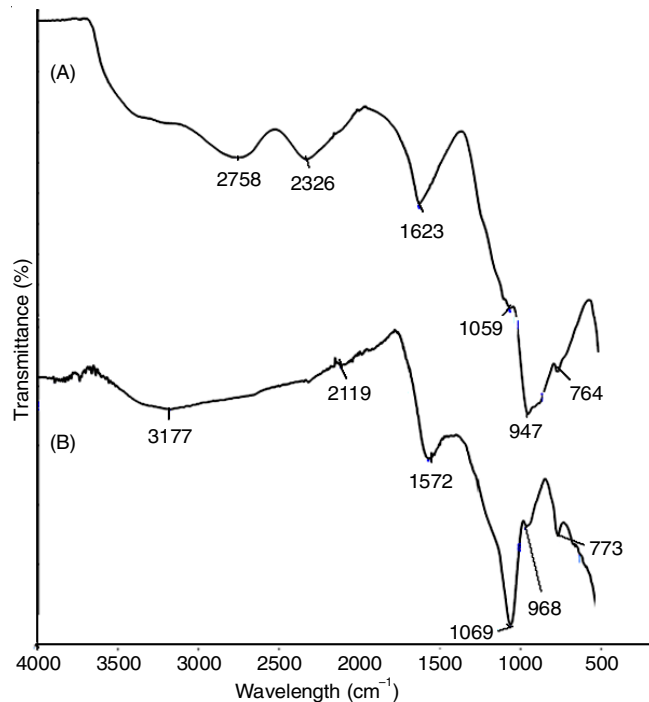


Fig. 5. FTIR spectra of activated carbon (A) the spectra of activated carbon (B) the spectra of activated carbon after nitric acid treatment

peak at 1069  $\text{cm}^{-1}$  is clearly influenced by the present acid as a extension of peak at 1059  $\text{cm}^{-1}$ . These peaks are attributed to the O-H or C-O vibration of oxygen-containing functional groups such as carboxylic acid. The peaks in 947-968  $\text{cm}^{-1}$  region are show C-H bending aromatic compound. The peaks obtained at 764-773  $\text{cm}^{-1}$  are assigned to C-H in out-of-plane bending at the edges of aromatic rings or assigned to C-halogen on the surface of activated carbon. The result of this data can be concluded that the effects of nitric acid treatment have reduced and shifted some peaks to extend the functional groups.

#### Adsorption study using activated carbon

**Effect of pH:** Adsorption of metal ions in aqueous solution onto activated carbon was affected by the solution pH. For initial reaction, the condition of reaction is set up using 0.5 g of activated carbon dosage, 100 mg/L of metal concentration and 45 min of contact time with the variable of pH lying between 3 and 10. The effects of pH on the removal of Pb(II) and Cr(VI) are shown in Fig. 6. It has been reported that solution pH plays important roles in the removal of cations or anions which occur in the range of pH 4-8. For Pb(II) ion, increasing of solution pH is followed by the increasing of adsorption capacity of metal ions and reaches equilibrium at pH 8. It was assumed that an increasing in solution pH releases more positive charges from the surface and more negative charges exist on the surface sites that can bind more Pb(II) ion. Conversely, for the Cr(VI) ion, increasing in solution pH produced more negative charges on the surface site and would be difficult to bind Cr(VI) ion existing as  $\text{HCrO}_4^-$  and as  $\text{CrO}_4^{2-}$ . This reason might describe the decreasing adsorption capacity of Cr(VI) during increasing in solution pH to pH 8 and increasing at pH 10 [14].

**Effect of adsorbent dosage:** The influence of adsorbent dosage on the adsorption capacity was investigated. The adsor-

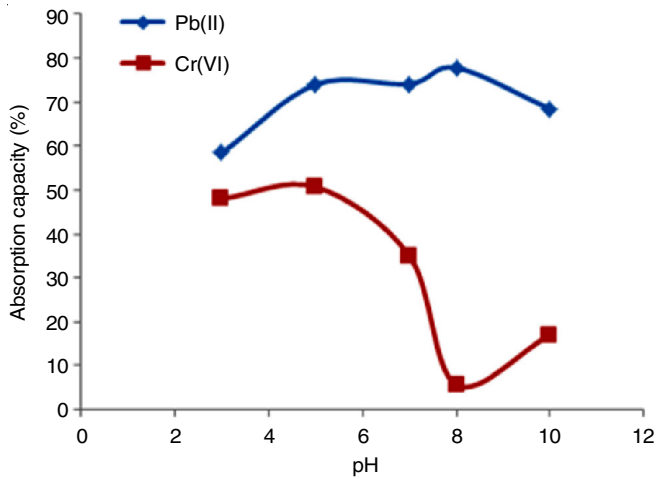


Fig. 6. Adsorption capacity of metal ions affected by different pH

ption capacity increases with an increasing adsorbent dosage. The reason is that increasing adsorbent dosage may enlarge the number of surface and active sites. It serves a large number of adsorbate accumulated on the surface for the adsorption process. Adsorption process can be described with three types of mechanisms: 1) by the anionic-cationic adsorption through the electrostatic interaction; 2) by the adsorbate-adsorbent interaction through porous structures; 3) by the combination of anionic-cationic adsorption and porous structures [15]. The adsorption capacity of Pb(II) and Cr(VI) is shown in Fig. 7. It is assumed that removal of Pb(II) and Cr(V) occurred through the combination of mechanisms. Lead(II) ion in solution can be directly adsorbed by the activated carbon. However, chromium adsorption in solution might have two forms Cr(VI) and Cr(III) ions that they can compete each other in adsorption process.

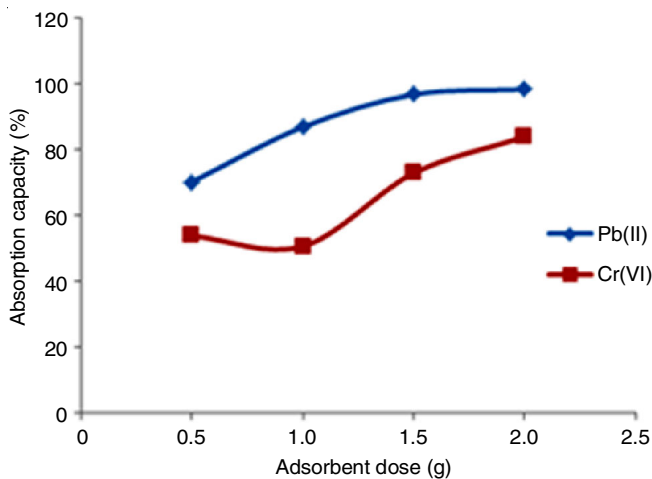


Fig. 7. Adsorption capacity of metal ions affected by different adsorbent dosages

**Effect of contact time:** The effects of contact time on the removal of Pb(II) and Cr(VI) by the activated carbon are presented in Fig. 8. For Pb(II), the efficiency of metal ions adsorption is almost plateau from 15 to 75 min. It illustrates that adsorption process has reached equilibrium at 30 min. It is assumed that all pores have been filled with Pb(II) ion. However, the adsorption of Cr(VI) significantly increases from 15 min and plateau after 60 min. Decreasing adsorption rate

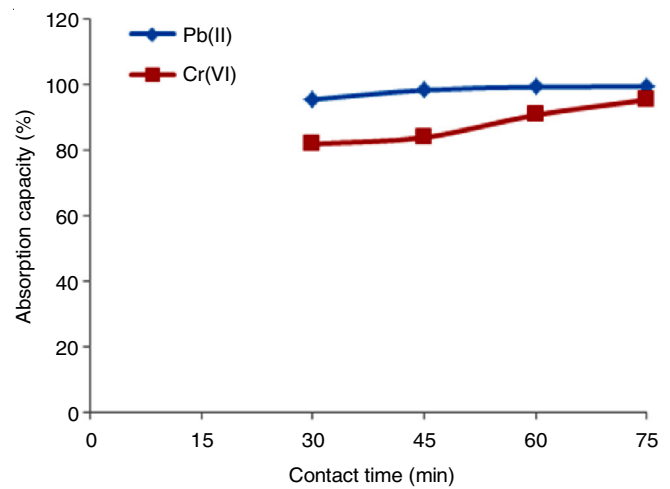


Fig. 8. Adsorption capacity of metal ions affected by different contact times

of the activated carbon might be due to a lower in number of pores or the pores are filled by the absorbed metals. The plateau curve indicates a lower adsorption, particularly toward the end of adsorption process.

**Effect of concentration:** The effect of Pb(II) and Cr(VI) concentration on the sorption onto activated carbon are shown in Fig. 9. The adsorption capacity of metal ions decreases with increasing concentration. It indicates a low sorption of metals in solution. It is assumed due to the insufficiently available pores in the activated carbon. In other words, all pores have been filled by the metal concentrations.

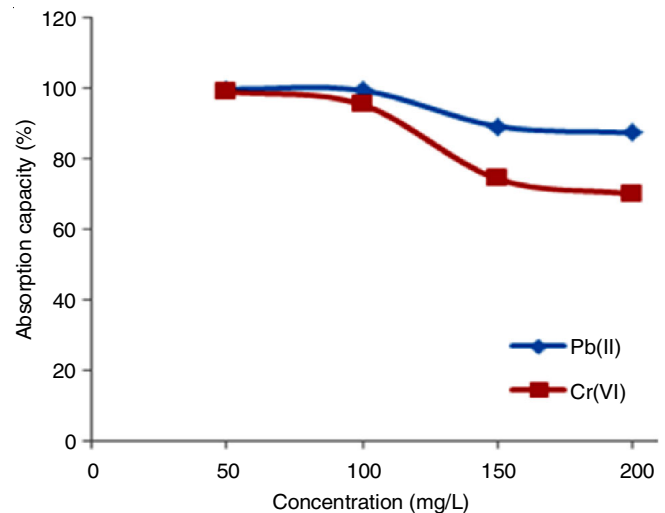


Fig. 9. Adsorption capacity of metal ions affected by different concentrations

**Adsorption isotherms:** The Freundlich isotherm shows correlation coefficient ( $R^2$ ) of 0.9019 and 0.9389 for Pb(II) and Cr(VI), respectively. The measurements of Langmuir isotherm have correlation coefficient,  $R^2$  of 0.9693 and 0.9767 for Pb(II) and Cr(VI), respectively. The maximum adsorption of Langmuir isotherm ( $q_m$ ) were obtained 4.1736 and 3.4200 mg/g for Pb(II) and Cr(VI), respectively. The adsorption capacity of Pb(II) using banana empty fruit bunch activated carbon is low, if it is compared with previous work such as activated carbon prepared from coconut shell, sea-buck stone *etc.* However, it shows better adsorption than activated carbon prepared

TABLE-2  
FREUNDLICH AND LANGMUIR ISOTHERMS FOR REMOVAL OF METAL IONS

Metal	Langmuir isotherm			Freundlich isotherm		
	Sorption capacity $q_m$ (mg/g)	Langmuir isotherm constant $K_L$ (L/mg)	Correlation coefficient $R^2$	Freundlich isotherm constant $K_F$	Adsorption intensity $n$	Correlation coefficient $R^2$
Pb(II)	4.1736	1.2119	0.9693	2.2867	5.4025	0.9019
Cr(VI)	3.4200	0.4058	0.9767	1.5642	5.2882	0.9389

from raw carbon nanotube [16,17]. The low adsorption capacity can be assumed that many of pore were closed by the unwanted particles. The completed parameters of equilibrium adsorption for the Freundlich and Langmuir isotherms are presented in Table-2. Applicability of the Freundlich and Langmuir isotherms can explain the ongoing adsorption process of Pb(II) and Cr(VI) ions onto activated carbon. The data of  $R^2$  values were fitted to show the Freundlich and Langmuir isotherms. The  $R^2$  value of Freundlich isotherm is higher than  $R^2$  values Langmuir isotherm. Specifically, the Freundlich isotherm is more favourable sorption for removal of Pb(II) and Cr(VI) ions onto activated carbon.

The value of adsorption intensity ( $n$ ) in the Freundlich isotherm can describe the degree of non-linearity between solution concentration and adsorption. If the value of  $n = 1$ , the adsorption is linear; if the value of  $n < 1$ , the adsorption is chemical adsorption and if  $n > 1$ , the adsorption is physical adsorption. If  $n$  value lies within in the range of 1-10, it is indicative a good physical adsorption process of metal ions onto activated carbon [17,18]. In this work, the  $n$  values in Freundlich isotherms are found of 5.4025 and 5.2882 for Pb(II) and Cr(VI), respectively (Table-2). The result suggested that the activated carbon from empty fruit bunch is more favourable absorbed through the Freundlich isotherm.

### Conclusion

In this paper, activated carbon was prepared from banana empty fruit bunch using phosphoric acid and under hydro-thermal carbonization. Characterizations of activated carbon like specific surface area, pore volume and pore size distribution including oxygen-containing functional groups signify the effectiveness of adsorbent. Adsorption behaviours of Pb(II) and Cr(VI) ions were evaluated with the Freundlich and Langmuir isotherms. The Freundlich isotherm is more favourable sorption compared to the Langmuir isotherm with the correlation coefficient ( $R^2$ ), 0.9767 and 0.9693 for Pb(II) and Cr(VI), respectively. The results obtained in this study suggested that banana empty fruit bunch can be considered as raw materials for production of activated carbon and efficiently used for removal of metal ions.

### ACKNOWLEDGEMENTS

The authors acknowledge the financial grants from Directorate of Research and Public Service (DPPM), Department of Chemistry, Faculty of Mathematics and Natural Sciences and Laboratory of Universitas Islam Indonesia. The authors also thank to all laboratory staffs for their support.

### REFERENCES

- H.A. Hegaz, *HBRC J.*, **9**, 276 (2013); <https://doi.org/10.1016/j.hbrcj.2013.08.004>.
- M.S. Abdel-Raouf and A.R.M. Abdul-Raheim, *J. Pollut. Effects Control*, **5**, 180 (2017); <https://doi.org/10.4172/2375-4397.1000180>.
- K.R.S. Harsha, M. Murthy, L. Udayasimha, Dharmaprakash and D. Rangappa, *Mater. Today: Proceed.*, **4**, 12321 (2017); <https://doi.org/10.1016/j.matpr.2017.09.166>.
- M.A. Barakat, *Arab. J. Chem.*, **4**, 361 (2011); <https://doi.org/10.1016/j.arabjc.2010.07.019>.
- Z. Yang, Z. Zhang, L. Chai, Y. Wang, Y. Liu and R. Xiao, *J. Hazard. Mater.*, **301**, 145 (2016); <https://doi.org/10.1016/j.jhazmat.2015.08.047>.
- A.O. Dada, A.P. Olalekan, A. Olatunya and A.O. Dada, *IOSR J. Appl. Chem.*, **3**, 38 (2012).
- M.K.B. Gratuito, T. Panyathanmaporn, N. Sirinuntawittaya, A. Dutta and R.A. Chumnanklang, *Bioresour. Technol.*, **99**, 4887 (2008); <https://doi.org/10.1016/j.biortech.2007.09.042>.
- P. Sugumaran, V. Priya Susan, P. Ravichandran and S. Seshadri, *J. Sustain. Energy Environ.*, **3**, 125 (2012).
- A. Arami-Niya, W.M.A.W. Daud and F.S. Mjalli, *Chem. Eng. Res. Design*, **89**, 657 (2011).
- S.M. Anisuzzaman, C.G. Joseph, W.M.A.W. Daud, D. Krishnaiah and H.S. Yee, *Int. J. Ind. Chem.*, **6**, 9 (2015); <https://doi.org/10.1007/s40090-014-0027-3>.
- M.B. Desta, *J. Thermodyn.*, **Article ID 375830** (2013); <https://doi.org/10.1155/2013/375830>.
- Y.S. Ho, *Polish J. Environ. Stud.*, **15**, 81 (2006).
- M.K. Rai, G. Shahi, V. Meena, R. Meena, S. Chakraborty, R.S. Singh and B.N. Rai, *Resour.-Effic. Technol.*, **2**(Suppl. 1), S63 (2016); <https://doi.org/10.1016/j.reffit.2016.11.011>.
- M.M. Rahman, M. Adil, A.M. Yusof, Y.B. Kamaruzzaman and R.H. Ansary, *Materials*, **7**, 3634 (2014); <https://doi.org/10.3390/ma7053634>.
- A. Tytlak, P. Oleszczuk and R. Dobrowolski, *Environ. Sci. Pollut. Res. Int.*, **22**, 5985 (2015); <https://doi.org/10.1007/s11356-014-3752-4>.
- E. Deliyanni, A. Arabatzidou, N. Tzoupanos and K.A. Matis, *Adsorpt. Sci. Technol.*, **30**, 627 (2012); <https://doi.org/10.1260/0263-6174.30.7.627>.
- E.A. Deliyanni, G.Z. Kyzas, K.S. Triantafyllidis and K.A. Matis, *Open Chem.*, **13**, 699 (2015); <https://doi.org/10.1515/chem-2015-0087>.
- A. Ozer and H.B. Pirincci, *J. Hazard. Mater.*, **137**, 849 (2006); <https://doi.org/10.1016/j.jhazmat.2006.03.009>.